AIDR 3D Enhanced — The latest hybrid model-based iterative dose reduction technology from Canon Medical

I. Hernandez-Giron, W. J. H. Veldkamp, J. Geleijns
Radiology Department,
Leiden University Medical Center (LUMC), The Netherlands

Introduction

Computed tomography has become one of the most popular diagnostic imaging techniques in medicine over the past decades. The number of CT studies performed worldwide is continuously increasing due to the wide range of clinical indications and the introduction of new clinical applications. This has had a positive impact on patients' diagnosis assessment and outcome but concerns about radiation dose to the patient continue to motivate the development of dose reduction technologies, such as iterative reconstruction. Iterative reconstruction is a powerful radiation dose reduction tool, dramatically reducing the magnitude of image noise. However, iterative reconstruction can result in image noise texture that looks over-smoothed or "plastic" in visual appearance compared to filtered back projection (FBP) reconstruction, especially at low doses. Figure 1 shows the differences in noise texture in images of a low contrast detectability phantom reconstructed with FBP (left) and two iterative reconstruction algorithms (middle and right). The new AIDR* 3D Enhanced from Canon Medical reduces radiation dose while remedying the problem of over-smoothed noise texture by improving the noise grain size to render images with a desirable noise texture appearance and improved spatial resolution[2].

* Adaptive Iterative Dose Reduction

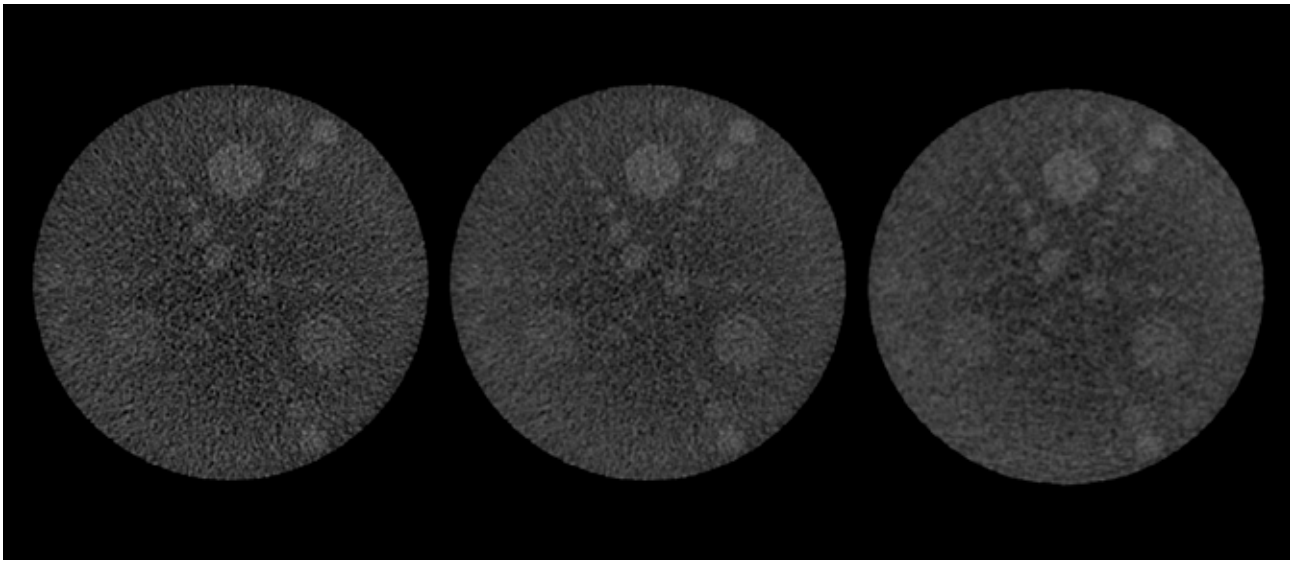

Figure 1 CT images of a low contrast detectability phantom reconstructed with filtered back projection (left) and two iterative reconstruction methods. It can be seen as some of the objects become blurred out in the right image, due to the over-smoothed noise texture.

AIDR 3D Enhanced is a model-based iterative dose reduction technique (Figure 2) combining three models acting on the acquired projection data. One model for the scanner, another for the statistical noise distribution and photon noise model (based on the Noise Power Spectrum). This enables to reduce the noise and streak artifacts, maintaining the spatial resolution and controlling the noise grain size. This is done by applying a low-frequency 3D filter in the raw data, producing a noise texture which has a finer grain size than that of the previous AIDR 3D algorithm. Then, to generate the final image, the number of iterations and blending ratio in the image data is optimized.

This paper compares the performance of the latest version of AIDR from Canon Medical called AIDR 3D Enhanced, with the previous version (AIDR 3D STD) and filtered back projection (FBP). Phantom and patient images were assessed in this comparison study. Quantitative image quality measurements, such as noise (measured as the standard deviation of pixel values) and Noise Power Spectrum (NPS) were performed[3-6]. Spatial resolution was also assessed visually with two phantoms, one with a distribution of line pair/cm gauge and the other containing high contrast disk-shaped targets or different diameters. Images of an anthropomorphic phantom and clinical patient images were also used for visual analysis, in particular for streaks and dark band artifacts due to photon starvation.

Material and methods and results

This section is comprised of three parts. The first one is based on objective measurements of image quality performed together with geometric phantoms; the second one is based on the visual comparison of images of an anthropomorphic thorax phantom, containing bronchi and vessels, for a clinical indication (ultra low dose CT thorax); the third one is a showcase of clinical patient images reconstructed with FBP, AIDR 3D and AIDR 3D Enhanced depicting artifact reduction and the differences in noise texture.

Phantom study and image quality measurements

Three geometric phantoms containing simple test objects were scanned on a Canon Medical Aquilion ONE GENESIS Edition CT system using a variety of protocols (described in detail in each subsection). The experiments were performed with a small water phantom, the Catphan phantom and the QRM-D100-3D phantom[7,8]. The phantom images were used to either illustrate visually the differences in noise texture between AIDR 3D Enhanced and AIDR 3D (STD) and FBP, respectively, or to apply objective quantitative image quality measurements.

The differences in noise texture were studied with a small water phantom (for a brain protocol) and with the uniformity module of the Catphan phantom (abdomen protocol). The differences in spatial resolution between the three algorithms were quantified with the high resolution module of the Catphan phantom (which contains patterns of high contrast line-pairs objects) and the QRM-D100-3D spatial resolution insert (with series of small drilled holes of known diameter and spacing).

Water phantom: Noise texture

The aim of this section is to show the perceptual differences in the noise texture ("graininess") and grain size and to estimate the noise variation. A small water phantom (16 cm diameter) was scanned using a brain protocol for a range of dose levels. The images were reconstructed with the three reconstruction methods.

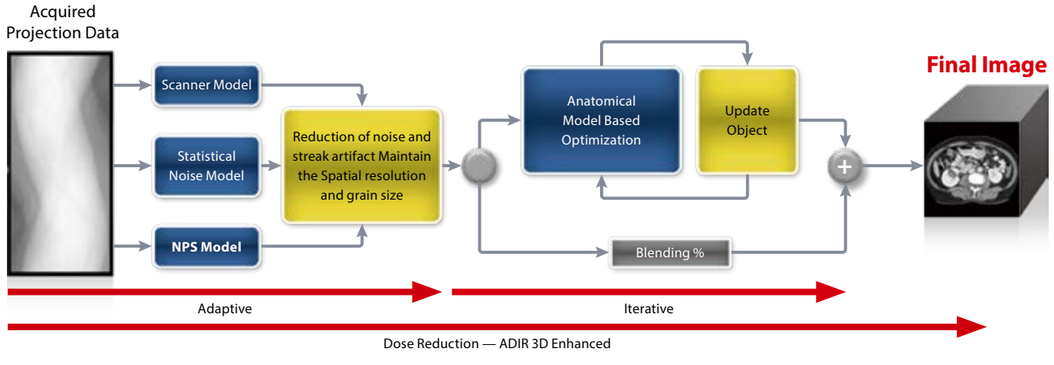

Figure 2 Diagram depicting the AIDR 3D Enhanced algorithm, including the raw data and image processing steps.

Figure 3 summarizes a selection of the reconstructed phantom images. It can be seen that the noise contains relatively more large-grain, visually-unappealing noise texture with AIDR 3D STD compared to AIDR 3D Enhanced. The noise grain size is smaller with AIDR 3D Enhanced. Noise was measured as the standard deviation (SD) of the pixel values inside a region of interest of 6 cm diameter taken on the phantom images. Comparing FBP with AIDR 3D STD, noise decreased by 74%, 65% and 56% (10-20-40 mAs, respectively). For AIDR 3D Enhanced, the noise reduction was 67%, 56% and 43%, respectively.

Catphan phantom

The Catphan® 500 phantom, widely used in quality control in CT, contains several modules which can be used to assess different aspects of image quality. In particular, the modules used in this study were the uniformity module, to measure the noise power spectrum, and the spatial resolution module.

Noise power spectrum (NPS)

The NPS represents the intensity of noise as a function of spatial frequency. The NPS contains information about the noise magnitude (area under the curve) and the noise texture (given by the shape of the curve). Images of the uniformity module of the Catphan phantom were analyzed to depict visually the differences in noise texture between the three reconstruction algorithms. Furthermore, the NPS was calculated over a 128 × 128 pixel extracted from the center of the phantom to quantify objectively the differences in the spatial frequency distribution of the noise[2,3,5]. The phantom was scanned with an abdominal protocol, modifying the tube current per rotation, and selecting two typical reconstruction filters for this body part.

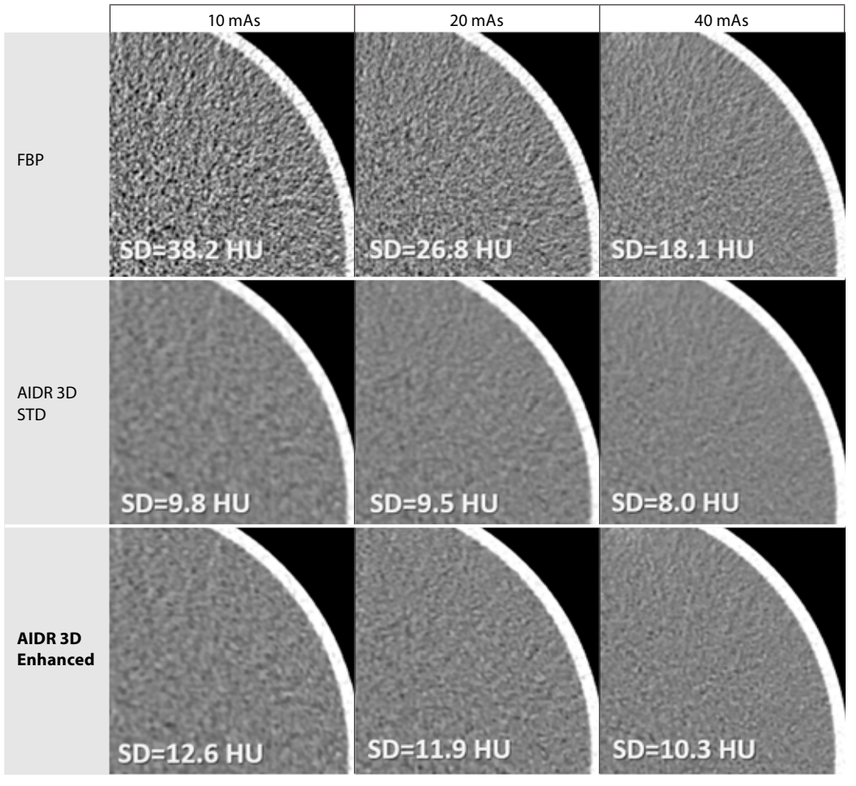

Figure 3 Small water phantom (16 cm diameter) scanned with 120 kV, 80 × 0.5 mm collimation, pitch standard (HP=0.813) and reconstructed as 0.5 mm slices and a dFOV=320 mm with a FC26 filter with FBP, AIDR 3D (STD) and AIDR 3D Enhanced for a range of dose levels (WL/WW=0/250 HU).

Figure 4 depicts the calculated NPS curves, averaged over 5 acquisitions in identical conditions, for the sets reconstructed with FBP, AIDR 3D STD and AIDR 3D Enhanced for a FC18 filter. Figure 5 depicts the NPS obtained for one separate acquisition (with a slightly higher mAs) and reconstructed with a different kernel (FC13). Samples of the images used in this study are shown on the right of figures 4 and 5, for the three reconstruction methods, to illustrate the perceived changes in noise texture visually.

It can be seen that for AIDR 3D STD and AIDR 3D Enhanced, the peak of the NPS is lower than for the traditional filtered back projection reconstructed images (lower maximum noise) for both kernels. As expected, the area under the NPS curve (noise magnitude) was also higher for FBP, followed by AIDR 3D Enhanced and AIDR 3D STD.

The texture of the noise also differs, for the two selected reconstruction kernels (FC13 and FC18), as it can be seen in the images (Figures. 4 and 5, right). The smaller grain size in AIDR 3D Enhanced is represented in the NPS curves: for higher frequencies, the noise is higher than with the previous version of AIDR 3D (STD), though it is still much lower than for FBP, whereas for low frequencies the curves are very similar for the two selected reconstruction kernels (FC13 and FC18). It has to be noted that these are radially rebinned and thus the high frequency differences between algorithms are more significant than they appear.

Spatial resolution

The Catphan phantom high resolution module contains a test gauge consisting of 21 groups of objects representing different line pairs per cm (lp/cm).

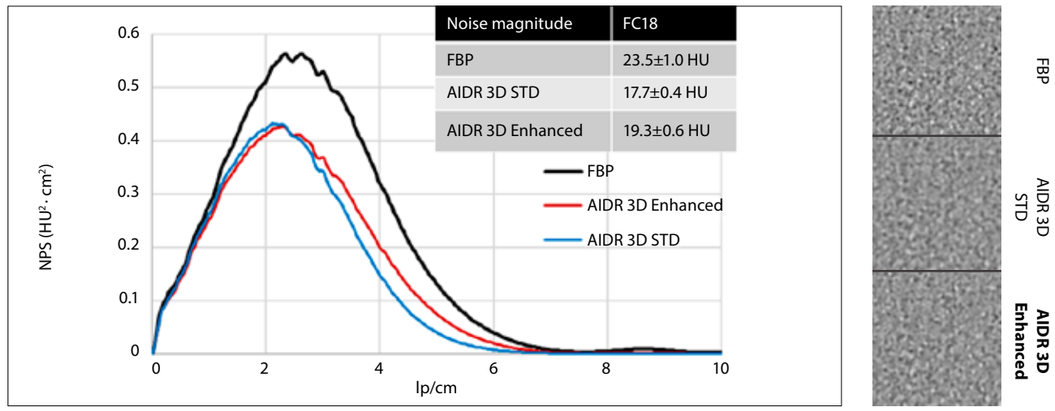

Figure 4 Noise power spectrum (NPS) measured over images of the Catphan phantom uniformity module, averaged over five acquisitions, each of them consisting of 48 slices. The selected protocol was 120 kV, 25 mAs, 80 × 0.5 mm collimation, pitch 0.813 and reconstructed as 1 mm slices and a dFOV=242 mm with a FC18 filter with FBP, AIDR 3D (STD) and AIDR 3D Enhanced. Samples of the images for each reconstruction algorithm (128 × 128 px²) are shown next to the graph (WL/WW=0/250 HU).

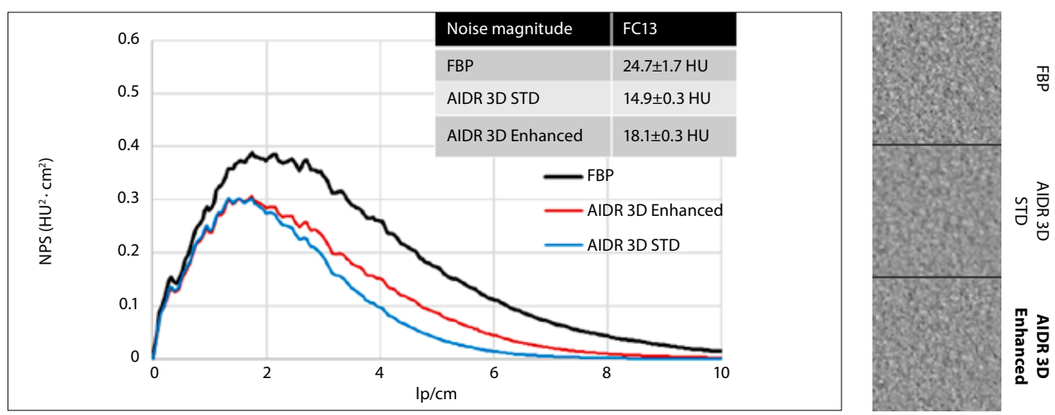

Figure 5 Noise power spectrum (NPS) measured over images of the Catphan phantom uniformity module, for one acquisition, consisting of 48 slices. The selected protocol was 120 kV, 30 mAs, 80 × 0.5 mm collimation, pitch 0.813 and reconstructed as 1 mm slices and a dFOV=242 mm with a FC13 filter with FBP, AIDR 3D (STD) and AIDR 3D Enhanced. Samples of the images for each reconstruction algorithm (128 × 128 px²) are shown next to the graph (WL/WW=0/250 HU).

Figure 6 depicts the groups of objects corresponding with 7, 8, 9, 10 and 11 lp/cm, respectively (corresponding to gap sizes of 0.071, 0.063, 0.053, 0.050 and 0.045 cm). It can be seen that AIDR 3D Enhanced rendered improved spatial resolution compared to AIDR 3D STD and FBP, as the groups of line pairs appear depicted sharper.

QRM-D100-3DSR spatial resolution phantom

The QRM-D100-3DSR spatial resolution insert contains a test pattern of drilled holes varying in diameter and spacing ranging from 4 mm (1.25 lp/cm) to 0.4 mm (12.5 lp/cm)[8]. The insert was scanned selecting a brain protocol and the acquisition and reconstruction settings shown in Figure 7. It can be seen that for both dose levels, AIDR 3D Enhanced outperformed FBP and AIDR 3D (STD) resolving groups of smaller objects better and sharply, even though the selected reconstruction filter (FC26) was the same.

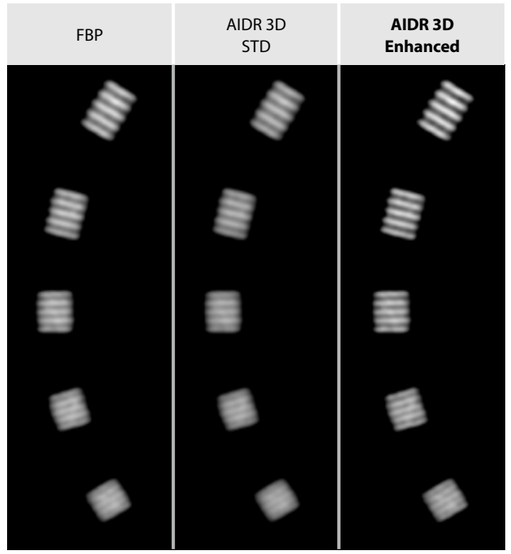

Figure 6 Images of the Catphan phantom high resolution module acquired with the following acquisition and reconstruction parameters: 120 kV, 60 mAs, 0.5 × 80 mm collimation, pitch standard (HP=0.813), cFOV=240 mm, FC13 reconstruction kernel, 0.5 mm slice thickness and spacing, dFOV=60 mmm (WL/WW=1000/1000 HU).

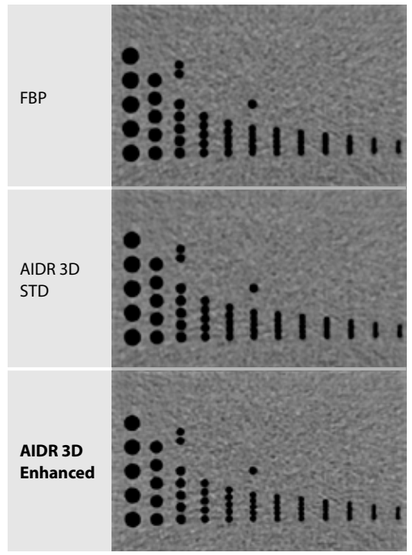

Figure 7 Images of the QRM-D100-3DSR phantom acquired with a brain protocol in a Canon Medical Aquilion ONE GENESIS Edition selecting 120 kV, 40 × 0.5 mm, HP Detail (HP=0.637), $CTDI_{vol}$ =6.5 mGy, and reconstructed with 0.5 mm as slice thickness and interval, FC26 reconstruction kernel.

Anthropomorphic phantom

An anthropomorphic phantom (Kyoto Kagaku CT Torso phantom CTU-41)[9] was scanned using a high resolution thorax protocol at various dose levels and reconstructed with three reconstruction methods (AIDR 3D Enhanced, AIDR 3D STD and FBP) to visually illustrate their differences. This phantom contains anatomical structures cast on synthetic materials that mimic the attenuation of tissue in the human body, such as bone, lungs with pulmonary vessels (up to the fourth bifurcations), and internal organs.

Figure 8 shows an example of the obtained images, for an extremely low dose (ultra low dose chest CT, $CTDI_{vol}$ =0.7 mGy). It can be seen that the streak artifacts present in the FBP reconstruction are mostly reduced with both AIDR 3D STD and AIDR 3D Enhanced. Regions of interest (A, B, C) were taken over the lung parenchyma (which is air in this phantom) and the heart. For this particular protocol and dose, noise, measured as the statistical deviation of the pixel values, was reduced in a factor 3 comparing FBP with AIDR 3D STD and AIDR 3D Enhanced for the lung parenchyma (ROI A) and in a factor 5 for the soft tissue (heart equivalent in the phantom, ROIs B and C).

Figure 8, also depicts the presence of streak artifacts, due to photon starvation. It has to be noted that the selected thorax protocol and dose was very low ($CTDI_{vol}$ =0.7 mGy). The undesired artifacts are especially noticeable in the FBP reconstruction at the top and bottom of the coronal view and at the bottom of the axial view. This undesired effect was reduced with AIDR 3D Enhanced.

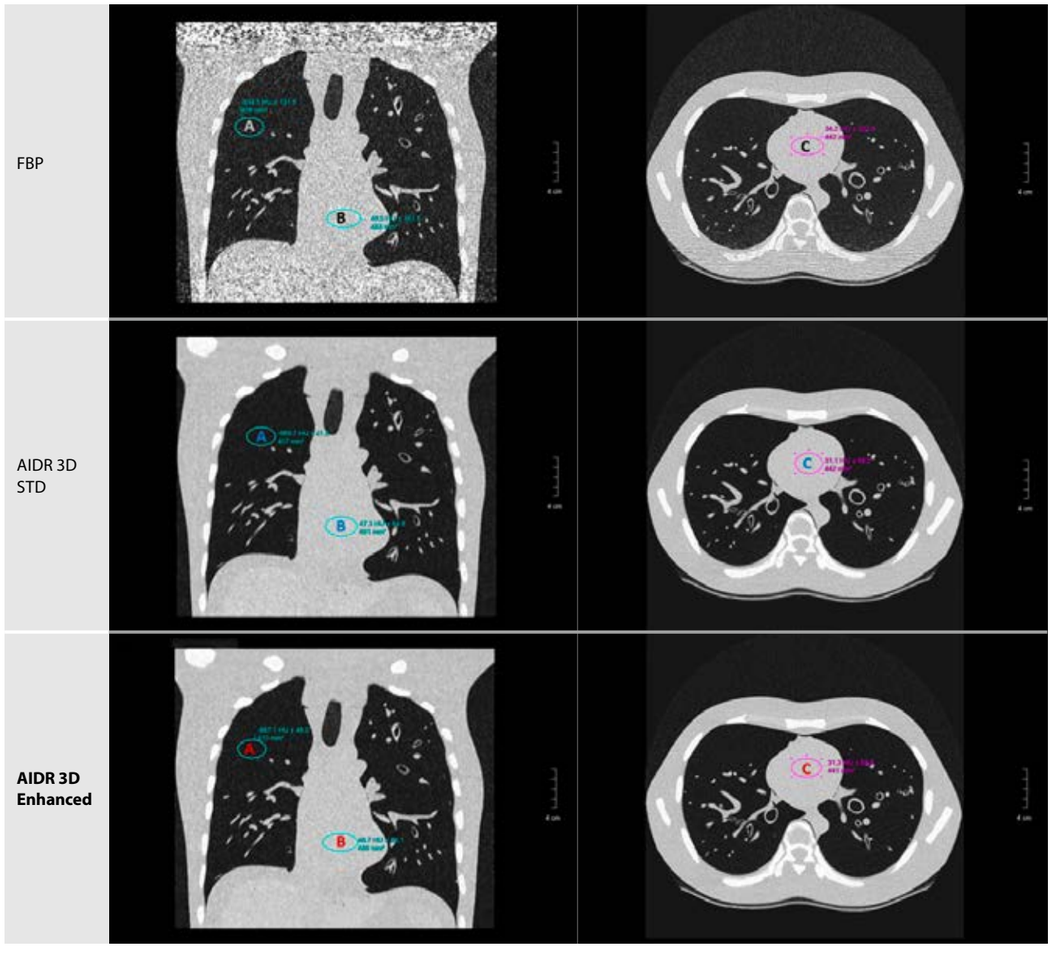

Figure 8 Images of the Kyoto Kagaku torso phantom acquired with a high resolution chest protocol in a Canon Medical Aquilion ONE GENESIS Edition selecting 120 kV, 40 × 0.5 mm, HP Detail (pitch=0.637), and reconstructed with 1 mm as slice thickness and interval, FC52 reconstruction kernel at a ultra-low dose ($CTDI_{vol}$ =0.7 mGy), (WL/WW=-400/1600 HU).

Figure 9 shows three zoomed in examples for the bronchi walls visibility in the phantom depending on the reconstruction method. It can be seen that some bronchi walls, which were not clearly visible with AIDR 3D STD, are depicted sharply with AIDR 3D Enhanced.

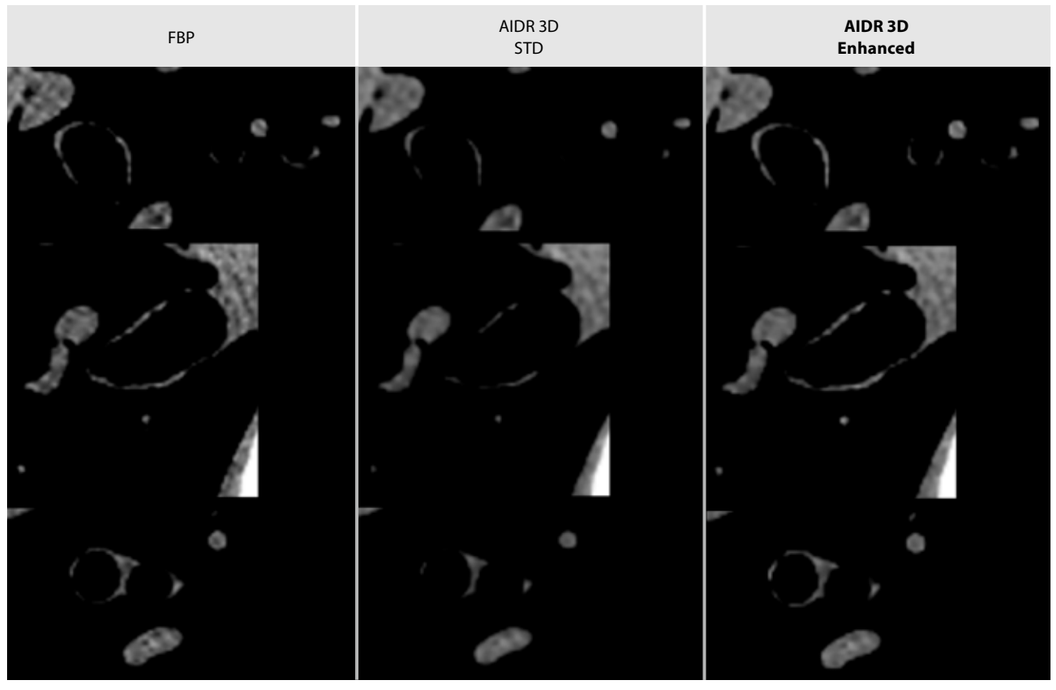

Figure 9 Examples of the visibility of the bronchi walls in the Kyoto Kagaku torso phantom acquired with a high resolution chest protocol in Aquilion ONE GENESIS Edition selecting 120 kV, 40 × 0.5 mm, HP Detail (pitch=0.637), and reconstructed with 1 mm as slice thickness and interval, FC18 reconstruction kernel for at a ultra-low dose ($CTDI_{vol}$ =0.7 mGy), (WL/WW=35/430 HU).

AIDR 3D Enhanced in the clinical setup

Dark band artifact reduction

AIDR 3D Enhanced reduces dark band artifacts when compared with filtered back projection (FBP) or the previous version of AIDR 3D. These artifacts can appear in body regions with big differences in attenuation between lateral and postero-anterior projections, such as shoulders or pelvis, due to photon starvation. An example of dark band artifact can be seen in Figure 10 depicting the shoulder area of a patient where the artifact is clearly visible on the image on the left, reconstructed with the previous version of AIDR 3D (STD) and not visible in the set of images reconstructed with AIDR 3D Enhanced (right), due to a better photon noise estimation (Figure 10).

Streak artifact reduction

AIDR 3D Enhanced reduces streak artifacts that can appear in the image due to lack of signal in the detector for certain projections. These artifacts can be related to the presence of high attenuation objects in certain X-ray beam path projections (such as dense bone in the pelvis, shoulders, the spine, or metal implants) or to the inherent attenuation of the patient when they have a high body mass index. An example of this undesired effect with an anthropomorphic phantom was shown in Figure 8: AIDR 3D Enhanced showed a clear improvement in image quality compared to images reconstructed with FBP for which the streaks were very apparent .

Figure 11 presents images related to a cardiac protocol reconstructed at 75% of the RR interval during the arterial phase for a patient with big BMI (acquisition at 135 kV). The top image was reconstructed with FBP and shows streak artifacts in the heart and the vertebra. The middle image shows AIDR 3D STD, for which part of the streaks have been removed. The bottom image with AIDR 3D Enhanced offers the best image quality of the three based on the absence of streaks, even compared with STD.

Noise texture

In section 2, a quantitative analysis was perform on the differences in noise texture of AIDR 3D Enhanced, AIDR 3D STD and FBP using geometric image quality phantoms. Figure 12 shows patient images related to the portal venous phase of an abdominal protocol to depict them qualitatively. Zoomed in sections are shown where it can be seen that AIDR 3D STD noise is more over-smoothed than for AIDR 3D Enhanced.

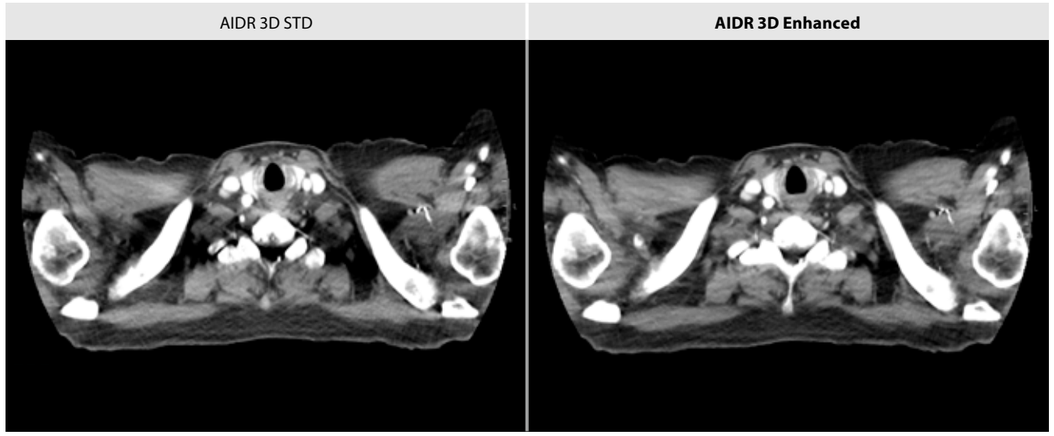

Figure 10 Patient images of the shoulder region, showing a dark band artifact (left) due to photon starvation. The artifact is reduced in the images reconstructed with AIDR 3D Enhanced (right), compared to the images reconstructed with AIDR 3D STD (left).

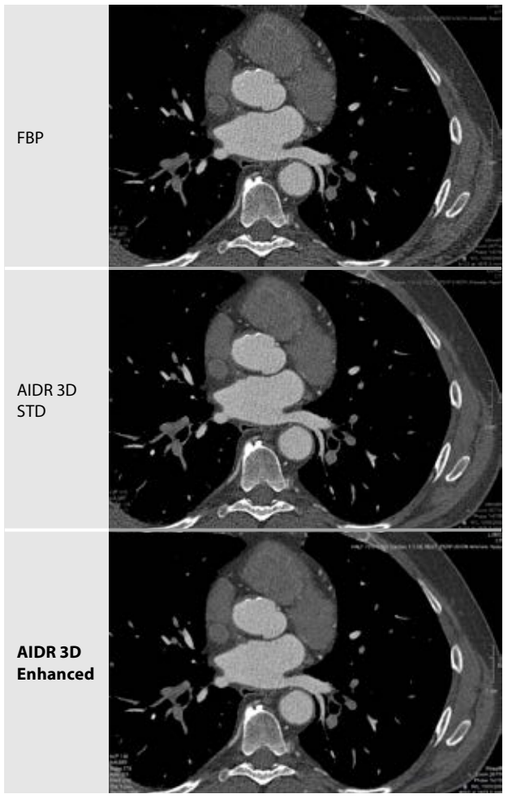

Figure 11 CT images of a cardiac protocol for a patient with high BMI, showing streak artifacts due to photon starvation. The artifact is reduced in the images reconstructed with AIDR 3D Enhanced (bottom) compared to the images reconstructed with AIDR 3D STD (middle) and FBP (top).

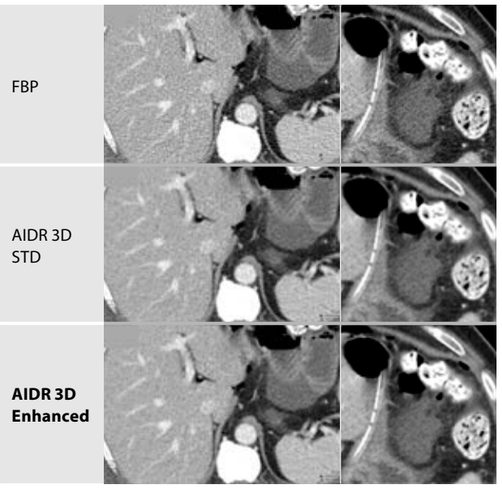

Figure 12 CT images of an abdominal protocol (portal venous phase) depicting noise texture differences between FBP (top), AIDR 3D STD (middle) and AIDR 3D Enhanced (bottom). On the right, part of another image of the same study has been zoomed in.

Conclusion

An overview of AIDR 3D Enhanced, the new model-based iterative reconstruction algorithm for dose reduction by Canon Medical, was presented in this paper. This algorithm renders a finer noise grain size and improves the detection of high contrast fine structures. Objective image quality metrics, such as NPS showed the changes in noise texture of AIDR 3D Enhanced compared to the previous generation of AIDR 3D STD, especially for high frequencies in the image. Images of an anthropomorphic phantom and clinical patient images were also used to depict the differences in visualization of structures in images acquired with different protocols and reconstructed with FBP, AIDR 3D STD and AIDR 3D Enhanced. AIDR 3D Enhanced also proved to be more effective in the reduction of dark band and streak artifacts, related to photon starvation, than AIDR 3D.

References

1. Geyer LL, Schoepf UJ, Meinel FG, Nance JW, Bastarrika G, Leipsic JA, et al. State of the art: Iterative CT reconstruction techniques. *Radiology* 2015;276(2):339-357.
2. Joemai RMS, Veldkamp WJH, Kroft LJM, Hernandez-Giron I, Geleijns J. Adaptive Iterative Dose Reduction 3D versus filtered back projection in CT: Evaluation of image quality. *AJR* 2013;201:1291-1297.
3. Boedeker KL, Cooper VN, McNitt-Gray MF. Application of the noise power spectrum in modern diagnostic MDCY. Part 1. Measurement of noise power spectra and noise equivalent quanta. *Phys Med Biol* 2007;52:4027-4046.
4. Joemai RMS, Geleijns J, Veldkamp WJH. Development and validation of a low dose simulator for computed tomography. *Eur Radiol* 2010;20:958-966
5. Solomon JB, Christianson O, Samei E. Quantitative comparison of noise texture across CT scanners from different manufacturers. *Med Phys* 2012;39:6048-6055.
6. Tack D, Kalra MK, Genevois PA, editors. *Radiation dose from multidetector CT,* 2nd ed. Springer-Verlag Berlin Heidelberg; 2012.
7. https://www.phantomlab.com/catphan-500
8. http://www.qrm.de/content/products/imagequality/D100-3DSR.htm
9. https://www.kyotokagaku.com/products/detail03/ph-4.html

CANON MEDICAL SYSTEMS CORPORATION
https://global.medical.canon

©Canon Medical Systems Corporation 2018. All rights reserved.
Design and specifications are subject to change without notice.
MCACT0334EA 2018-12 CMSC/D/Printed in Japan

Canon Medical Systems Corporation meets internationally recognized standards for Quality Management System ISO 9001, ISO 13485.
Canon Medical Systems Corporation meets the Environmental Management System standard ISO 14001.

Aquilion ONE, Aquilion ONE GENESIS and Made for Life are trademarks of Canon Medical Systems Corporation.

Catphan is a registered trademark of The Phantom Laboratory.

Made For life